Effects of second order chemical reaction on MHD forced convection Cu, Ag, and Fe$_3$O$_4$ nanoparticles of Jeffrey Nanofluid over a moving plate in a porous medium in the presence of heat source/sink

B. Reddappa[*], R. Geetha

Department of Mathematics, School of Advanced Sciences, Kalasalingam Academy of Research and Education (Deemed to be university), Anand Nagar, Krishnankoil, Tamil Nadu, India

Article

ABSTRACT

The objective of the current research is to determine how a second order chemical reaction will affect the magnetohydrodynamic flow of a water-based Jeffrey nanofluid containing Copper (Cu), Silver (Ag), and Ferrous Ferric Oxide (Fe$_3$O$_4$) nanoparticles over a flowing stream embedded in a porous medium in the presence of a heat source/sink. The governing system of PDEs is converted into nonlinear ODEs using the similarity

transformation approach, and these nonlinear ODEs are then resolved using MATLAB's built-in solver, bvp4c. In a single plot of three nanoparticles and tables, the output of the nanofluid velocity, temperature, and concentration are displayed for the included material properties as well as the related engineering physical parameters like coefficient of skin friction and rate of heat and mass transfer. This model has been rather successfully validated. The results indicate that the nanofluid $\theta(\eta)$ and $\Box(\eta)$ profiles decline as λ_1 increases, while this behavior is opposite for the distributions of $f'(\eta)$. The kinetic energy of fluid particles decelerates because of the high viscosity. The study demonstrates the significance of three nanoparticles in the disciplines of biocompatibility engineering and medicines. Additionally, these nanoparticles are utilized in engineering, physics, space technology, operations involving high temperatures and cooling, pharmaceuticals, biosensors, paints, cosmetics, conductive coatings, and medical devices.
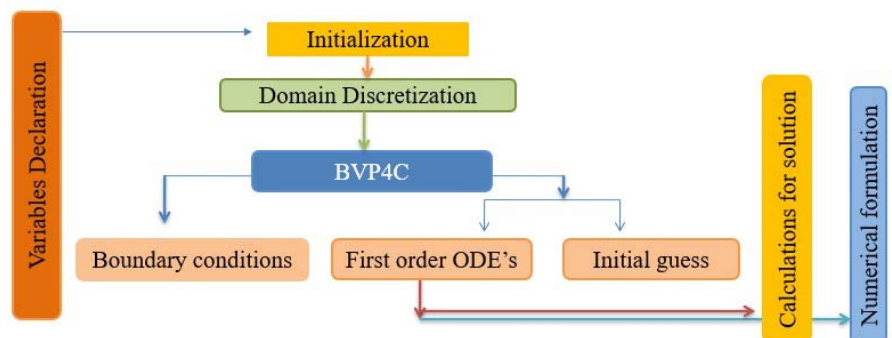
Keywords: MHD flow; Nanofluids; Porous medium; Heat and mass transfer; Second order chemical reaction

INTRODUCTION

Nanofluids have recently been shown to have a significant impact on a variety of industries, and fundamental studies in field of engineering, science, and technology. It is due to their numerous uses and applications, including oil recovery, enhanced heat transfer, nanofabrication and drug delivery, as well as contemporary cooling techniques.[1] As a consequence, a thorough examination of the characteristics of heat and flow transmission has been conducted. Researchers have developed a number of techniques to increase the ability of convective heat transmission in fluids, including the suspension of nanoparticles in basic fluids including water, kerosene, ethylene glycol, human blood, and carbon nanotubes (CNTs). Aaiza et al.[2] examined the movement of a nanofluid including different nanoparticle morphologies. Researchers have developed hypotheses about a wide range of extraordinary properties that affect how nanofluids behave in an effort to completely understand their properties.[3] It is well known that the presence of a nanofluid with the MHD effect can enhance the heat transfer capabilities of an electrically conductive fluid. In line with the idea of MHD and porous medium of nanofluid, some significant new research about heat transfer through convective boundary conditions, heat source/sink, and chemical interaction of nanofluid have been reported in literature.[4,5] The limited research

Journal of Integrated Science and Technology

J. Integr. Sci. Technol., 2024, 12(3), 762   Pg 1

indicates that the problem significantly affects the cooling process physically.

The ambiguity of the boundary layer structure at two-channel walls that are inclined at a fixed angle to the flow of an incompressible, viscous fluid via a divergent/convergent channel is one of the major problems in fluid dynamics. Earlier studies on these difficulties were conducted by Jeffery[6] and Hamel.[7] The existence of fluid volume sources and sinks at the intersection of two channel walls causes flow in certain situations, which can result in either a divergent or a convergent flow. For the velocity field, Pohlhausen[8] discovered an analytical convergent flow solution, while Millsaps and Pohlhausen[9] looked at the temperature distribution. Distinguished researchers Harison[10], Tollmien[11], Noether[12], and Dean[13] examined a few of this flow's interesting properties. Bhattacharyya and Layek[14] conducted more research on the MHD boundary layer of a power-law non-Newtonian fluid in a diverging permeable channel with suction/injection. The MHD flow of a water-based Nanofluid in a stretchable/shrinkable convergent/divergent channel with thermal radiation effects was studied by Dogonchi and Ganji[15].

Due to their many applications, particularly in granule storage, metal processing, insulation devices, geothermal systems, heat-switch devices, straining processes, catalytic reactors, etc., fluid flow and heat transfer in porous media merit special attention (Mukhopadhyay and Layek[16], Mukhopadhyay et al.[17]). The flow of a water-based nanofluid containing gyrotactic bacteria via a horizontal flat plate in a porous media was studied by Aziz et al.[18]. The rotating flow of nanofluid over a plate in a porous media in the presence of a magnetic field, a chemical reaction, and heat radiation was further studied by Ramana Reddy et al.[19]. Chakraborty et al.[20] recently discussed the effects of heat radiation on an Ag-water nanofluid flow across a plate in a non-Darcy porous media. In the open literature, there aren't many studies on nanofluid flows in porous media.

It is well known that the magnetic field and the effects of chemical reactions have an impact on flow and heat transfer rates. They are used in a wide range of industrial, medical, and environmental applications. It is also acknowledged that they alter the way boundary layer flow behaves. Because of the addition of these features, studying fluid movement becomes more interesting and realistic. Zangooee et al.[21] looked at the MHD nanofluid flow between two revolving, stretchable discs. Titanium dioxide and Gallic oxide nanoparticles were widely distributed in the base fluid (water). In order to take advantage of the characteristics of heat transmission, they employed radiative heating and Joule to assess the flow. Aleem et al.[22] have investigated the MHD nanofluid flow via an accelerating vertical plate whose height is infinite. Additionally, they made advantage of Newtonian heating and chemical reaction effects. They investigated the five various types of nanoparticles while using water as the basic fluid. Krishna and Chamkha also addressed the MHD nanofluid flow problem[23]. Along with employing the perturbation technique, they looked into the Nusselt and Sherwood numbers to resolve the problem. Additionally, recent studies have covered the magnetic effects in nanofluid flow, according to certain useful publications.[24-40]

The current study is focused on the second order chemical reaction on the magnetohydrodynamic flow of a water-based Jeffrey nanofluid containing Copper, Silver, and Ferrous Ferric Oxide nanoparticles over a moving stream embedded in a porous medium in the presence of a heat source/sink, and is motivated by the literature review mentioned above. MATLAB's built-in solver, bvp4c, is used to numerically solve the boundary layer equations, and the results are displayed graphically. The novel findings from this study will be useful in a variety of nanotechnology and nanostructure sectors.

DESCRIPTION OF MATHEMATICAL PROBLEM

Let us have a look at a two-dimensional, constant-velocity U_w, laminar forced convective flow of nanofluid across a flat surface that is flowing either in the same direction as or in opposition to the free stream U_∞. The x-axis runs perpendicular to the surface, while the y-axis runs vertically, perpendicular to the surface. The magnetic field B is applied in the transverse direction of the flow (see Figure. 1). The water-based nanofluid in this example, which contains nanoparticles of Copper, Silver, and Ferrous Ferric Oxide, is in thermal equilibrium and does not slide between the particles.
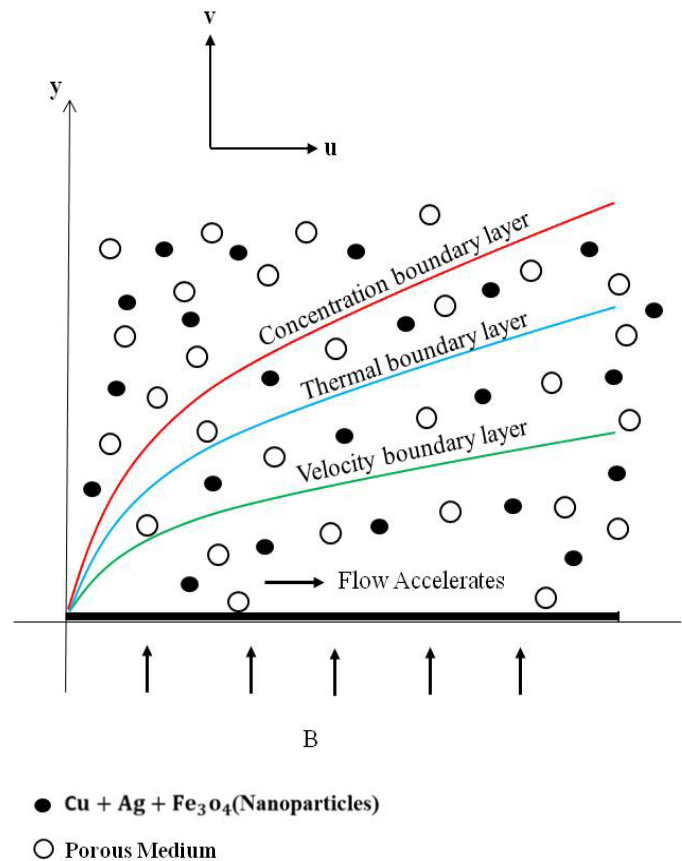
Figure 1. Geometry of the problem.

Given below are the boundary layer equations that control flow[41]

$$\frac{\partial u}{\partial x} + \frac{\partial v}{\partial y} = 0. \qquad (1)$$

$$u\frac{\partial u}{\partial x} + v\frac{\partial u}{\partial y} = \frac{v_{nf}}{1+\lambda_1}\frac{\partial^2 u}{\partial y^2} - \frac{\sigma B^2 u}{\rho_{nf}} - \frac{v_{nf}}{k_1}(u - u_\infty). \qquad (2)$$

$$u\frac{\partial T}{\partial x} + v\frac{\partial T}{\partial y} = \frac{K_{nf}}{(\rho c_p)_{nf}}\frac{\partial^2 T}{\partial y^2} - \frac{1}{(\rho c_p)_{nf}}\frac{\partial q_r}{\partial y} + \frac{Q}{(\rho c_p)_{nf}}(T - T_\infty). \qquad (3)$$

$$u\frac{\partial C}{\partial x} + v\frac{\partial C}{\partial y} = D\frac{\partial^2 C}{\partial y^2} + D_1\frac{\partial^2 T}{\partial y^2} - C_r(C - C_\infty)^2. \qquad (4)$$

The velocity components in the x and y directions are denoted by u and v, respectively; $\quad v_{nf} = \frac{\mu_{nf}}{\rho_{nf}}$ is the kinematic viscosity of the nanofluid $k_1 = k_0 x$ is the Darcy permeability of the porous medium; k_0 is the initial permeability, λ_1 is the Jeffrey parameter and μ_{nf} is the viscosity of the nanofluid. Now, for nanofluids ρ_{nf} denotes the density of the nanofluid; T denotes the temperature; k_{nf} represents the thermal conductivity of the nanofluid; and the specific heat capacitance of the nanofluid is denoted by $(\rho c_p)_{nf}$; $Q = \frac{Q_0}{x}$ is the heat generation or absorption coefficient, $Q > 0$ implies heat generation, $Q < 0$ represents heat absorption. D is the specifies diffusivity, and D_1 is the coefficient that signifies the contribution to mass flux through temperature gradient, C_r chemical reaction parameter and σ is electrical conductivity of the fluid.

The effective fluid properties are given by

$$\rho_{nf} = (1 - \phi)\rho_f + \phi\rho_s;$$

$$\frac{k_{nf}}{k_f} = \frac{2k_f + k_s - 2\phi(k_f - k_s)}{2k_f + k_s + \phi(k_f - k_s)}; \qquad \mu_{nf} = \frac{\mu_f}{(1-\phi)^{2.5}};$$

$$(\rho c_p)_{nf} = (1 - \phi)(\rho c_f)_f + \phi(\rho c_p)_s$$

Furthermore, ϕ is the solid volume fraction; μ_f denotes the dynamic viscosity of the basic fluid, ρ_f, and ρ_s are the densities of the base fluid and nanoparticles, respectively; k_f and k_s are the thermal conductivities of the base fluid and nanoparticles, respectively.

The following form can be used to express the proper boundary conditions:

$$u = U_w(x), v = -v_w(x), T = T_w(x), C = C_w(x)$$

at $y = 0$; $u \rightarrow U_\infty$, $T \rightarrow T_\infty$, $C \rightarrow C_\infty$ as $y \rightarrow \infty$. (5)

where

$$q_r = -\frac{4\sigma}{3k^*}\frac{\partial T^4}{\partial y}. \qquad (6)$$

$$T^4 \approx 4T^4_\infty - 3T^4_\infty. \qquad (7)$$

$$\frac{\partial q_r}{\partial y} = \frac{16\sigma^* 3T^3_\infty}{3k^*}\frac{\partial^2 T}{\partial y^2}. \qquad (8)$$

$T_w = T_\infty + ax^n$, $C_w = C_\infty + bx^n$, where a and b are constants.

$v_w = -\frac{1}{2}V_0\sqrt{\frac{v_f U}{x}}$ is the suction / injection velocity.

METHOD OF SOLUTION

Let us now introduce the stream function ψ as

$u = \frac{\partial \psi}{\partial y}, v = -\frac{\partial \psi}{\partial x}$ and consider the following similarity transformations:

$$\theta = \frac{T - T_\infty}{T_w - T_\infty}, h = \frac{C - C_\infty}{C_w - C_\infty}, \eta = y\sqrt{\frac{U}{2v_f x}},$$

$$R_{e_x} = \frac{Ux}{v_f}, \quad B = B_0 x^{-1/2}, \quad u = Uf'(\eta),$$

$$v = U\left(\frac{\eta f'(\eta) - f(\eta)}{\sqrt{2R_{e_x}}}\right).$$

Where ψ is stream function and η is similarity variable.

Using the above similarity transformations, the equations (2)-(4) are reduced to

$$\frac{1}{(1-\phi)^{2.5}\left(1-\phi+\phi\left(\frac{\rho_s}{\rho_f}\right)\right)}f''' + ff''(1 + \lambda_1) - 2\frac{M(1+\lambda_1)}{\left(1-\phi+\phi\left(\frac{\rho_s}{\rho_f}\right)\right)}f' -$$

$$2\frac{K(1+\lambda_1)}{(1-\phi)^{2.5}\left(1-\phi+\phi\left(\frac{\rho_s}{\rho_f}\right)\right)}(f' - \beta) = 0. \qquad (9)$$

$$\frac{\frac{k_{nf}}{k_f}}{\left(1-\phi+\phi\left(\frac{(\rho c_p)_s}{(\rho c_p)_f}\right)\right)}\theta''\left(1 + \frac{4R}{3}\right) + \Pr[f\theta' - 2nf'\theta +$$

$$2\frac{\lambda}{\left(1-\phi+\phi\left(\frac{(\rho c_p)_s}{(\rho c_p)_f}\right)\right)}\theta(\eta)] = 0. \qquad (10)$$

$$h'' - Sc[2nf'h - fh' + Krh^2] + Sr\theta'' = 0. \qquad (11)$$

The following are the flow's relevant boundary conditions:

$$f(\eta) = S, \qquad f'(\eta) = 1 - \beta, \qquad \theta(\eta) = 1,$$

$$h(\eta) = 1 \ at \ \eta = 0.$$

$$f'(\eta) = \beta, \ \theta(\eta) = 0, \ h(\eta) = 0 \ as \ \eta \rightarrow \infty. \qquad (12)$$

Where $S = -\frac{v_0}{\sqrt{2}}$ is the suction $(v_0 > 0)$ *blowing* $(v_0 < 0)$ parameter; $\beta = \frac{U_\infty}{U}$ is the velocity ratio parameter. For $0 < \beta < 1$, the plate and the fluid move in the same direction and when $\beta < 0 \ or \beta > 1$, they move in the opposite directions, $M = \frac{\sigma B_0^2}{U\rho_f}$ is the magnetic parameter, $\lambda = \frac{Q_0}{(\rho c_p)_f U}$ is heat source $(\lambda > 0)$ / sink $(\lambda < 0)$ parameter, $K = \frac{1}{D_{ax}R_{e_x}} = \frac{v_f}{k_0 U}$ is the parameter of the porous medium, $Pr = \frac{v_f((\rho c_p)_f}{k_f}$ is the Prandtl number, $\lambda = \frac{Q_0}{(\rho c_p)_f U}$ is heat source $(\lambda > 0)$ / sink $(\lambda < 0)$ parameter, $Sc = \frac{v_f}{D}$ is the Schmidt number, $\qquad Sr = \frac{D_1(T_w - T_\infty)}{D(C_w - C_\infty)}$ is the Soret number,

$R = \frac{4\sigma^* T^3_\infty}{k^* k_{nf}}$ is the radiation parameter, and

$Kr = \frac{C_r x(C_w - C_\infty)}{U}$ is the rate of reaction parameter.

Journal of Integrated Science and Technology

J. Integr. Sci. Technol., 2024, 12(3), 762   Pg 3

RESULTS AND DISCUSSION

In this investigation, we have taken into account three different types of nanoparticles: Copper (Cu), Silver (Ag), and Ferrous Ferric Oxide (Fe_3O_4) in water (H_2O) based nanofluid (using Table1) for two-dimensional steady laminar flow of an electrically conducting nanofluid over a Porous Medium in the Presence of Heat Source/Sink. The impact of heat generation or absorption coefficient, porosity, magnetic field, radiation, chemical reaction, and Soret nanoparticles of Cu, Ag, and in water (H_2O) based nanofluid have all been taken into account through the graphs for velocity, temperature, and concentration. The modified non-linear equations (9) through (11) have been solved under the boundary conditions (12) using the MATLAB-built tool "bvp4c." During numerical calculations, the values of default physical parameters are $M = 1.0$; $Pr = 0.7$; $K = 0.4$; $\beta = 1.3$; $Sc = 1.0$; $Kr = 0.2$; $n = 0.3$; $\lambda_1 = 0.1$; $R = 0.1$; $\lambda = 0.4$; $S = 0.1$; $\phi = 0.03$ and otherwise stated.

Figures. 2(a-c) exhibit the exact effects of λ_1 for Cu, Ag and Fe_3O_4 in water based nanofluid on velocity $(f'(\eta))$, temperature $(\theta(\eta))$, and concentration profiles $(h(\eta))$. It is pretty clear that $\theta(\eta)$ and $h(\eta)$ declines as λ_1 increases, while this behavior is opposite for the distributions of $f'(\eta)$. The kinetic energy of fluid particles decelerating because of the high viscosity.
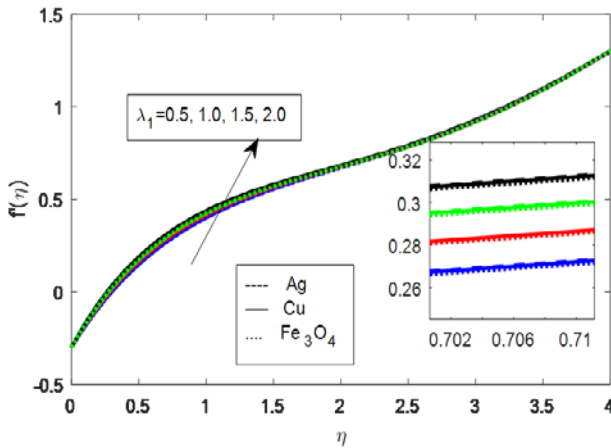
Figure 2(a). Variation of λ_1 on velocity.
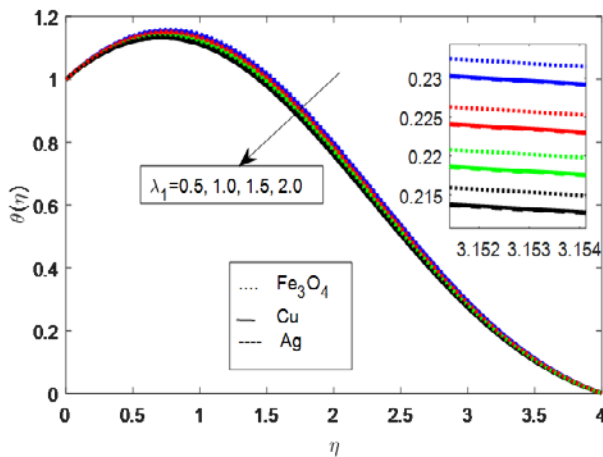
Figure 2(b). Variation of λ_1 on temperature.
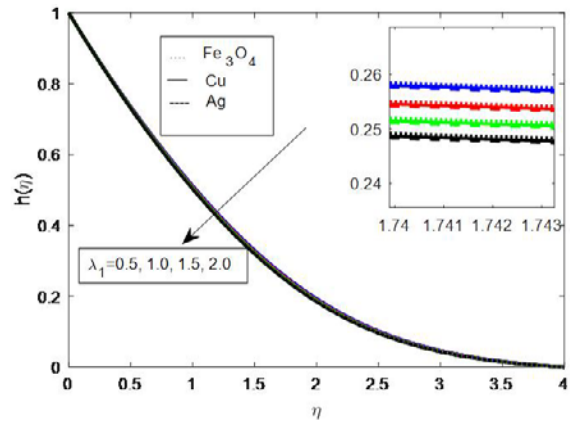
Figure 2(c). Variation of λ_1 on concentration

Figures. 3(a-c) highlight the impact of magnetic field (M) for Cu, Ag and Fe_3O_4 in water based nanofluid on velocity $(f'(\eta))$, temperature $(\theta(\eta))$, and concentration profiles $(h(\eta))$. Increasing M, leads to accelerate the nanofluid $\theta(\eta)$ and $h(\eta)$, while this behavior is opposite for the distributions of $f'(\eta)$. It is discovered that the velocity profile is significantly reduced by the magnetic field. This is due to the retarding-type force, or Lorentz force, which is created when a transverse magnetic field is applied perpendicular to the x-axis, along which fluid flow is expected to occur. Lorentz force tends to decelerate fluid particles, which results in a drop in velocity profile. Moreover, Ag nanoparticle gives rise to $\theta(\eta)$ and $h(\eta)$, followed by Cu and Fe_3O_4 in the boundary layer and therefore, they are accelerated due to the effect of M.
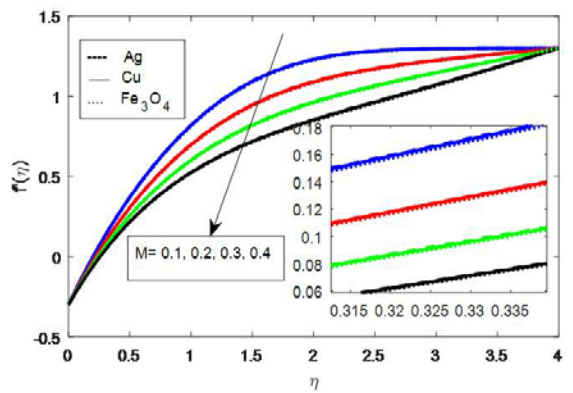
Figure 3(a). Variation of M on velocity
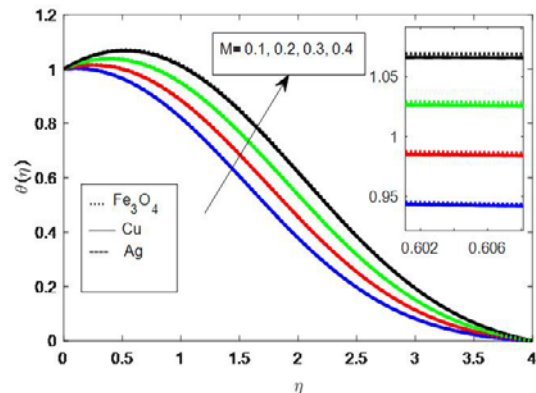
Figure 3(b). Variation of M on temperature

Journal of Integrated Science and Technology

J. Integr. Sci. Technol., 2024, 12(3), 762   Pg 4
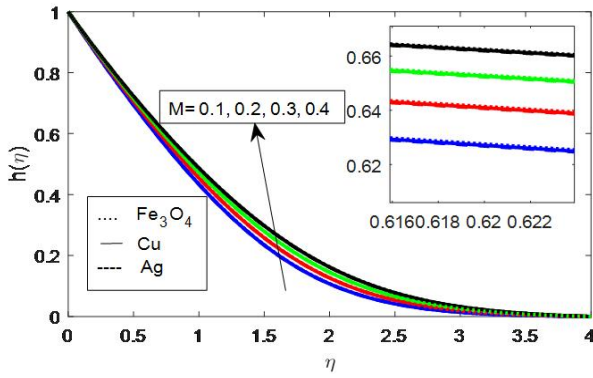
Figure 3(c). Variation of M on concentration

Figure 4(c). Variation of ϕ on concentration.

The effect of the nanoparticle volume fraction ϕ on velocity, temperature and concentration profiles are shown in Figures. 4(a-c). Due to the increase in the nanoparticle volume fraction, velocity increases. Ag–water nanofluid shows a higher velocity compared to Cu–water and Fe_3O_4 –water nanofluid. Due to increase in ϕ, temperature and concentration profiles decreases. Fe_3O_4 – water nanofluid exhibits a higher temperature compared to Cu–water and Ag–water nanofluid.
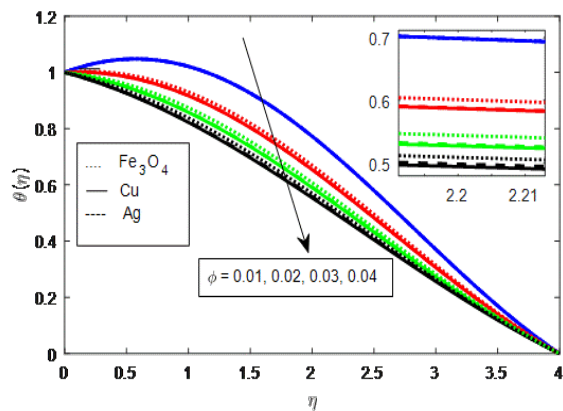
Figures.5(a-c) demonstrate the effect of porosity parameter (K) on $f'(\eta)$, $\theta(\eta)$ and $h(\eta)$ distributions of the Cu, Ag and Fe_3O_4 in water based nanofluid. The $f'(\eta)$ distributions are rises with increasing K. This is due to the presence of a porous medium that diminishes the resistance to the flow causing an increase in the $f'(\eta)$ profile. Fluid temperature and concentration profiles are decreases with the augmentation of the parameter K of porous medium. The thermal boundary layer and concentration boundary layer thickness are decreases.

Figure 4(a). Variation of ϕ on velocity
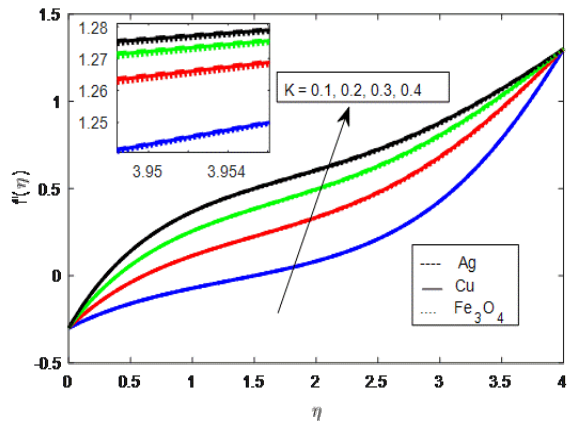
Figure 5(a). Variation of K on velocity

Figure 4(b). Variation of ϕ on temperature
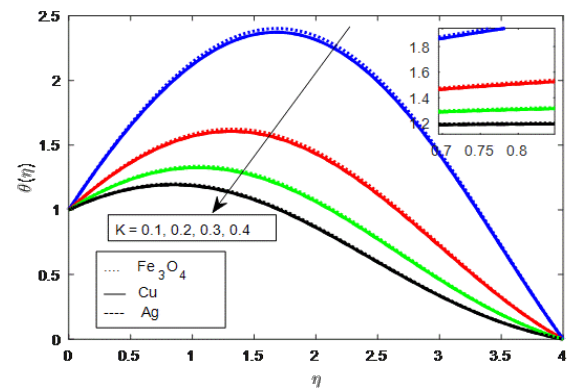
Figure 5(b). Variation of K on temperature

Journal of Integrated Science and Technology

J. Integr. Sci. Technol., 2024, 12(3), 762   Pg 5
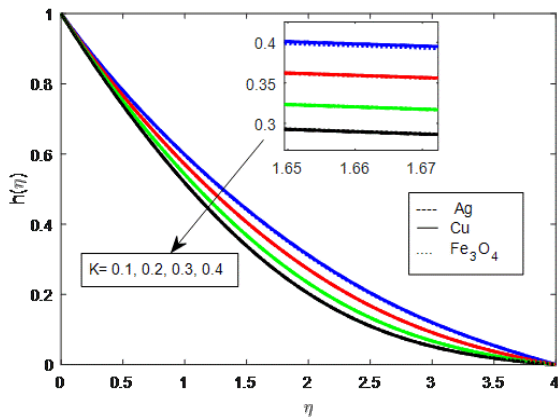
Figure 5(c). Variation of K on concentration.

Figures 6(a-c) illustrate the $f'(\eta)$, $\theta(\eta)$ and $h(\eta)$ profiles on suction/ blowing parameter (S), for the water based nanoparticles Fe_3O_4, Cu, Ag. It is found that the $\theta(\eta)$ and $h(\eta)$ for nanoparticles decreases due to increase of ($S > 0$), while this effect is opposite for the profiles of $f'(\eta)$.
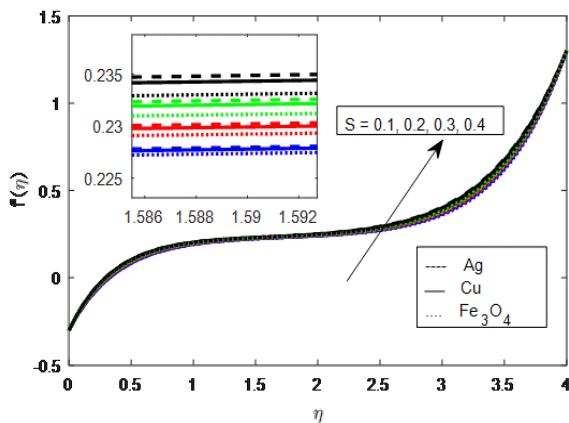
Figure 6(a). Variation of S on velocity
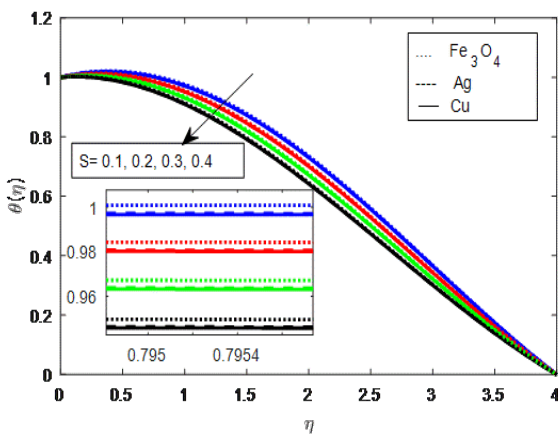
Figure 6(b). Variation of S on temperature
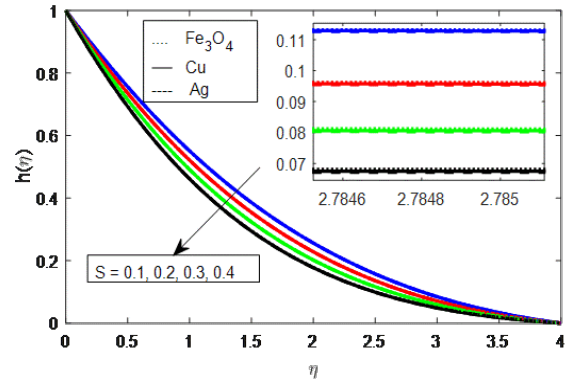
Figure 6(c). Variation of S on concentration

Figures. 7(a-b) describes the impact of R on temperature and concentration fields for the water based nanoparticles Fe_3O_4, Cu and Ag. Which depicts the flow temperature declines because the transfer of thermal energy from fluid region to the upper wall elevates with higher values of R, while this effect is opposite for the profiles of $h(\eta)$.
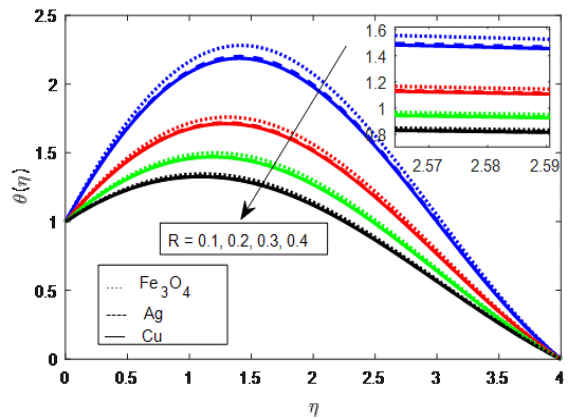
Figure 7(a). Variation of R on temperature
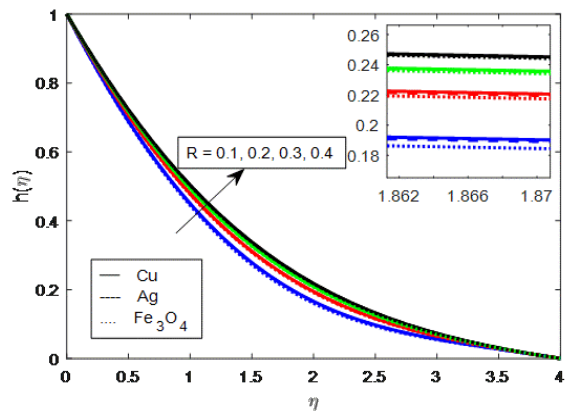
Figure 7(b). Variation of R on concentration

Figures. 8(a-b) describes the impact of heat source ($\lambda > 0$) / sink ($\lambda < 0$) parameter on temperature and concentration fields for the water based nanoparticles Fe_3O_4, Cu, Ag. Which depicts the

flow temperature increases for $(\lambda > 0)$ However, when temperature changes directly with the power-law exponent n (> 0), no temperature overshoot is detected for the upper branch solution, but temperature overshoot is noted for the lower branch solution. The profiles of $h(\eta)$, however, experience the inverse of this impact.
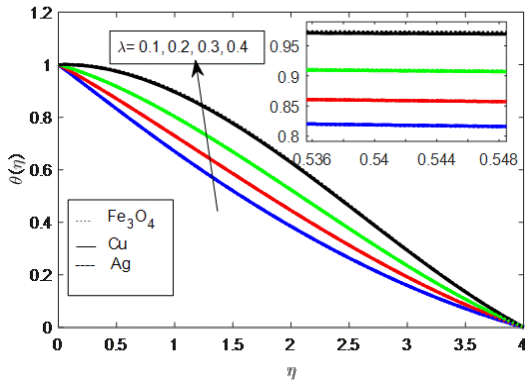
Figure 8(a). Variation of λ on temperature
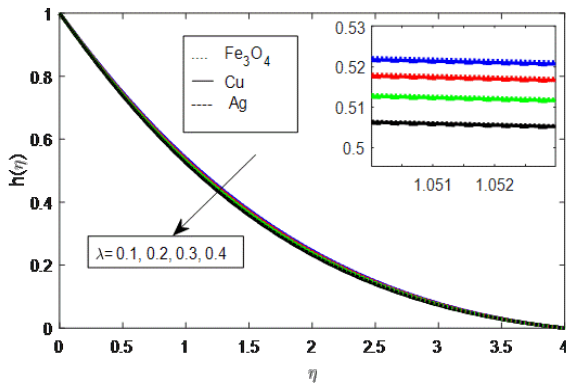
Figure 8(b). Variation of λ on concentration

Figures. 9 and 10 describe the effects of the power-law exponent (n) and Prandtl number (Pr) on temperature profiles for the water based nanoparticles Fe_3O_4, Cu, Ag. It is observed that temperature decreases with increasing values of n, that is no temperature overshoot is noted and whereas an increasing function of Prandtl number.
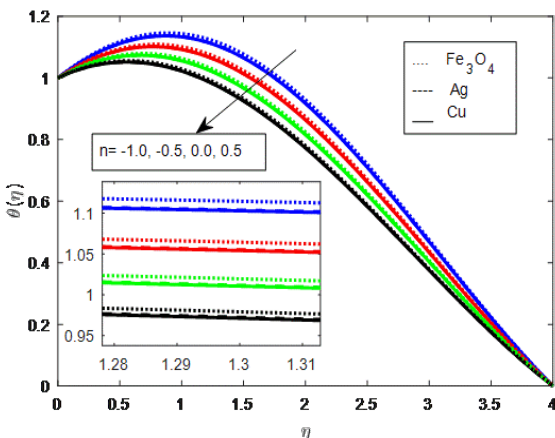
Figure 9. Variation of n on temperature.
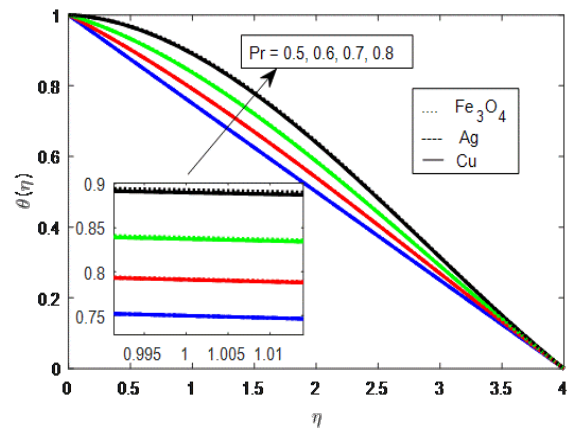
Figure 10. Variation of Pr on temperature

Figures. 11-13 explore the impacts of the parameters Sc, Kr, Sr on nanofluid concentration profiles for the water based nanoparticles Fe_3O_4, Cu and Ag. It is observed that concentration profiles decreases with increasing values of Sc, Kr, Sr.
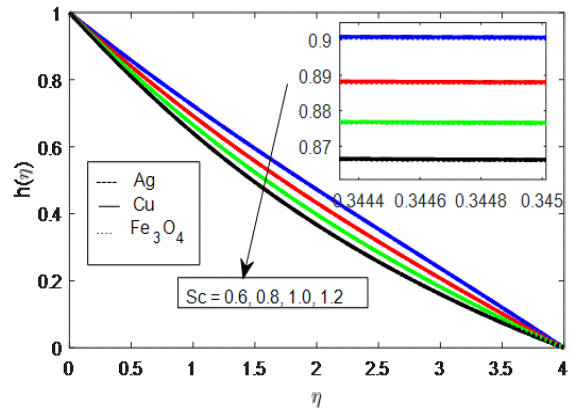
Figure 11. Variation of Sc on concentration
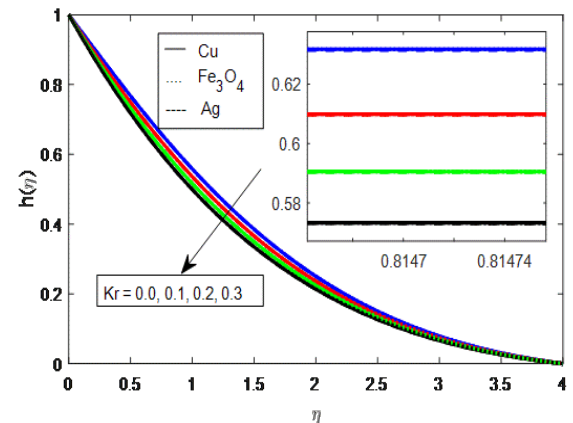
Figure 12. Variation of Kr on concentration.

Table 2 compares the present results which are in a good agreement with the earlier findings by Cortell [42]. Table 3 provides the values for the skin friction coefficient, heat and mass transfer rate for various physical parameters for the Cu- water based nanoparticles.

Journal of Integrated Science and Technology

J. Integr. Sci. Technol., 2024, 12(3), 762   Pg 7
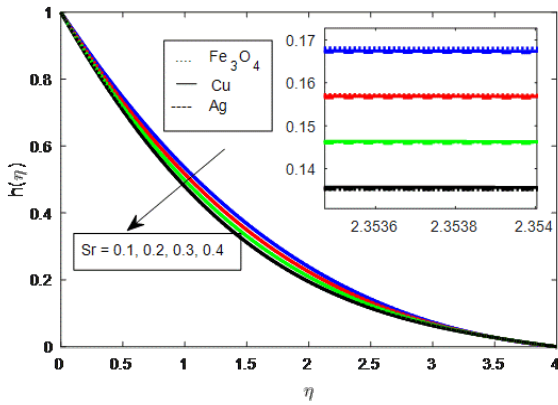
Figure 13. Variation of Sr on concentration

Table 2: Comparison of velocity gradient $f''(0)$ for a nonporous flat surface in the absence of porous medium with the results of [42] for $\phi = \lambda_1 = M = 0$

β	$f''(0)$	
	Cortell [42]	Present results
0.0	−0.627547	−0.627553
0.1	−0.493711	−0.493781
0.2	−0.363308	−0.363351
0.3	−0.237132	−0.237142
0.4	−0.115777	−0.115803

Table 1: Thermo physical properties of water, Copper, Silver and Ferrous Ferric Oxide

Physical quantity	Properties		
	$\rho\left(kg/m^3\right)$	$C_p\left(J/kg\ K\right)$	$k\left(W/m\ K\right)$
Water (H$_2$O)	997.1	4179	0.613
Copper (*Cu*)	8933	385	401
Silver (*Ag*)	10500	235	429
Ferrous Ferric Oxide (Fe$_3$O$_4$)	5180	670	9.7

Table 3: Skin friction coefficient, rate of heat and mass transfer for *Cu* - water base fluid

λ_1	M	K	β	ϕ	S	R	Pr	n	λ	Sc	Kr	Sr	$f''(0)$	$-\theta'(0)$	$-\phi'(0)$
0.1													-2.055368	0.906608	1.156753
0.2													-2.094128	0.907422	1.157963
	0.1												-2.162639	0.912375	1.164956
	0.2												-2.133568	0.910845	1.162753
		0.5											-2.157903	0.909211	1.160482
		0.6											-2.257982	0.911720	1.164178
			1.4										-2.326033	0.897589	1.142039
			1.5										-2.593370	0.888450	1.127253
				0.01									-2.038246	0.900322	1.156195
				0.03									-2.055368	0.906608	1.156753
					0.1								-2.055368	0.906608	1.156753
					0.2								-2.154216	0.938547	1.210204
						0.1							-2.055368	0.906608	1.156753
						0.2							-2.055368	0.916531	1.155774
							0.6						-2.055368	0.920070	1.155424
							0.7						-2.055368	0.906608	1.156753
								0.2					-2.055368	0.900735	1.149195
								0.3					-2.055368	0.906608	1.156753
									0.3				-2.055368	0.945194	1.153000
									0.5				-2.055368	0.867422	1.160565
										0.5			-2.055368	0.906608	1.084520
										1.0			-2.055368	0.906608	1.156753
											0.1		-2.055368	0.906608	1.133778
											0.3		-2.055368	0.906609	1.179307
												0.1	-2.055368	0.906608	1.156753
												0.2	-2.055368	0.906608	1.165971

CONCLUSIONS

The nanoparticles of Copper, Silver and Ferrous Ferric Oxide used in this study have many applications and uses across a wide range of fields. *Ag*- nanoparticles are increasingly employed in antimicrobial agents, consumer and industrial electronics, healthcare and personal care items, consumer goods, coatings for medical devices, the pharmaceutical sector, optical sensors, cosmetics, food, and orthopedics, among other things. *Ag*-nanoparticles have also made progress in the treatment of angiogenesis-related disorders including cancer. A potential nanoparticle for contemporary study, Fe$_3$O$_4$ is inexpensive and biocompatible. It is employed in the creation of vaccines and antibodies as well as in gene therapy, medication delivery, and cell labeling. Due to their excellent electrical and thermal conductivity and inexpensive price, *Cu*- nanoparticles are frequently utilized in optical, magnetic, and sensory devices. The MATLAB Build Solver bvp4c is used to numerically solve the converted nonlinear ODE. Important conclusions of the study include:

(i). The nanofluid $\theta(\eta)$ and $h(\eta)$ profiles decline as λ_1 increases, while this behavior is opposite for the distributions of $f'(\eta)$. The kinetic energy of fluid particles decelerate because of the high viscosity.

(ii). Increasing M, leads to acceleration of the nanofluid $\theta(\eta)$ and $h(\eta)$, while this

behavior is opposite for the distributions of $f'(\eta)$. It is found that magnetic field has a prominent reducing effect on the velocity profile.

(iii). Increase in the nanoparticle volume fraction (ϕ), the fluid velocity increases. Ag – water nanofluid shows a higher velocity compared to Cu – water and Fe_3O_4 – water nanofluid. Due to increase in ϕ, temperature and concentration profiles decreases.

(iv). The velocity profile is mounting with a raise of K. Fluid temperature and concentration profiles decreases with the augmentation of the parameter K of porous medium.

(v). With an increase in Sc, Kr and Sr, the nanofluid concentration profiles declines.

NOMENCLATURE

a, b	are constants
u	Velocity component in the x direction
v	Velocity component in the y direction
T	Dimensional temperature of the Nanofluid
C	Nanoparticle concentration
C_∞	Nanoparticle Concentration o f the free stream
C_w	Concentration at the surface
c_p	Specific heat capacity at constant pressure
D	Specifies diffusivity
D_1	Coefficient that signifies the contribution to mass flux through temperature gradient
T	Dimensional temperature of the Nanofluid
T_w	Temperature at the surface
T_∞	Temperature of the free stream
B_0	Magnetic field strength
$f'(\eta)$	Non dimensional velocity
S	Suction/blowing
Q	Heat generation or absorption coefficient
$h(\eta)$	Non-dimensional concentration
C_r	Dimensional chemical reaction parameter
Kr	Non-dimensional chemical reaction parameter
M	Non-dimensional Magnetic parameter
Pr	Prandtl number
Sc	Schmidt number
Sr	Soret number
R	Radiation parameter
k_1	Darcy permeability of the porous medium
K	Porosity parameter
q_r	Radiative heat flux

Greek Symbols

λ_1	Jeffrey parameter
$\theta(\eta)$	Non-dimensional temperature
η	Similarity variable
λ	Heat source / sink parameter
σ	Electrical conductivity
ϕ	Solid volume fraction of nanoparticles
α_{nf}	Thermal diffusivity
μ_{nf}	Viscosity of the nanofluid

ρ_{nf}	Density of the nanofluid
μ_f	Viscosity of the base fluid
β	velocity ratio parameter
$(\rho c_p)_f$	Heat capacity of the base fluid
$(\rho c_p)_s$	Effective heat capacity of a nanofluid
ψ	Stream function
ρ_f	Density of the base fluid
ρ_s	Density of nanoparticles
k_f	Thermal conductivity of base fluid
k_{nf}	Thermal conductivity of nanofluid
k_s	Thermal conductivity of nanoparticles

Subscripts

∞	Condition at the free stream
w	Condition at the surface
f	Base fluid
s	Nanoparticle
n_f	Nanofluid

CONFLICT OF INTEREST STATEMENT

The authors declare no conflict of interest..

REFERENCES AND NOTES

1. A.K. Prasad, S. Madanagurusamy. Recent advances in Materials development and design for Gas Sensing applications. *J. Mater. Nanosci.* **2022**, 9 (1), 1–2.
2. G. Aaiza, I. Khan, S. Shafie. Energy Transfer in Mixed Convection MHD Flow of Nanofluid Containing Different Shapes of Nanoparticles in a Channel Filled with Saturated Porous Medium. *Nanoscale Res. Lett.* **2015**, 10 (1), 1–14.
3. S.U.S. Choi. Enhancing thermal conductivity of fluids with nanoparticles. *Am. Soc. Mech. Eng. Fluids Eng. Div. FED* **1995**, 231, 99–105.
4. M.M. Rashidi, N. Vishnu Ganesh, A.K. Abdul Hakeem, B. Ganga. Buoyancy effect on MHD flow of nanofluid over a stretching sheet in the presence of thermal radiation. *J. Mol. Liq.* **2014**, 198, 234–238.
5. N.S. Elgazery. Nanofluids flow over a permeable unsteady stretching surface with non-uniform heat source/sink in the presence of inclined magnetic field. *J. Egypt. Math. Soc.* **2019**, 27 (1), 1–26,
6. G.B. Jeffery. The Two-Dimensional Steady Motion of a Viscous Fluid. *Nelineinaya Din.* **2009**, 29 (172), 101–109.
7. G. Hamel. Spiralförmige Bewegungen zäher Flüssigkeiten. *Jahresbericht der Dtsch. Math.* **1917**, 25, 34–60.
8. V.E. Pohlhausen. Berechnung der Eigenschwingungen statiisch besiimmter Fachwerke. *Zeitsclirilt fiir rtngewatidte Mdthemstik und Mech.* **1921**, 1 (1), 28–42.
9. K. Millsaps, K. Pohlhausen. Thermal Distributions in Jeffery-Hamel Flows Between Nonparallel Plane Walls. *J. Aeronaut. Sci.* **1953**, 20 (3), 187–196.
10. W.T. Harrison. The Pressure in a Viscous Liquid Moving Through a Channel with Diverging Boundaries. In *Proc. Camb. Phil. Soc.*; **1920**; Vol. 19, pp 307–312.
11. W. Tollmien. Gnenzschichtheoric Handbuch der Exper imental Physik. *Akadeneisahe Verlagsgesellschaft* **1921**, 4 (1), 241.
12. F. Noether. Handbuch der physikalischen und technischen Mechanik. *Nature* **1934**, 133 (3361), 480–480.
13. W.R. Dean. LXXII. Note on the divergent flow of fluid. *London, Edinburgh, Dublin Philos. Mag. J. Sci.* **1934**, 18 (121), 759–777.
14. K. Bhattacharyya, G.C. Layek. MHD boundary layer flow of dilatant fluid in a divergent channel with suction or blowing. *Chinese Phys. Lett.* **2011**, 28 (8), 84705.

15. A.S. Dogonchi, D.D. Ganji. Investigation of MHD nanofluid flow and heat transfer in a stretching/shrinking convergent/divergent channel considering thermal radiation. *J. Mol. Liq.* **2016**, 220, 592–603.

16. S. Mukhopadhyay, P.R. De, K. Bhattacharyya, G.C. Layek. Forced convective flow and heat transfer over a porous plate in a Darcy-Forchheimer porous medium in presence of radiation. *Meccanica* **2012**, 47 (1), 153–161.

17. S. Mukhopadhyay, P.R. De, K. Bhattacharyya, G.C. Layek. Forced convective flow and heat transfer over a porous plate in a Darcy-Forchheimer porous medium in presence of radiation. *Meccanica* **2012**, 47 (1), 153–161.

18. A. Aziz, W.A. Khan, I. Pop. Free convection boundary layer flow past a horizontal flat plate embedded in porous medium filled by nanofluid containing gyrotactic microorganisms. *Int. J. Therm. Sci.* **2012**, 56, 48–57.

19. J.V.R. Reddy, V. Sugunamma, N. Sandeep, C. Sulochana. Influence of chemical reaction, radiation and rotation on MHD nanofluid flow past a permeable flat plate in porous medium. *J. Niger. Math. Soc.* **2016**, 35 (1), 48–65.

20. T. Chakraborty, K. Das, P.K. Kundu. Ag-water nanofluid flow over an inclined porous plate embedded in a non-Darcy porous medium due to solar radiation. *J. Mech. Sci. Technol.* **2017**, 31 (5), 2443–2449.

21. M.R. Zangooee, K. Hosseinzadeh, D.D. Ganji. Hydrothermal analysis of MHD nanofluid (TiO2-GO) flow between two radiative stretchable rotating disks using AGM. *Case Stud. Therm. Eng.* **2019**, 14.

22. M. Aleem, M.I. Asjad, A. Shaheen, I. Khan. MHD Influence on different water based nanofluids (TiO2, Al2O3, CuO) in porous medium with chemical reaction and newtonian heating. *Chaos, Solitons and Fractals* **2020**, 130 (109437).

23. M.V. Krishna, A.J. Chamkha. Thermo-diffusion, chemical reaction, Hall and ion slip effects on MHD rotating flow of micro-polar fluid past an infinite vertical porous surface. *Int. J. Ambient Energy* **2022**, 43 (1), 5344–5356.

24. M. Gholinia, M.E. Hoseini, S. Gholinia. A numerical investigation of free convection MHD flow of Walters-B nanofluid over an inclined stretching sheet under the impact of Joule heating. *Therm. Sci. Eng. Prog.* **2019**, 11, 272–282.

25. B. Souayeh, M.G. Reddy, P. Sreenivasulu, et al. Comparative analysis on non-linear radiative heat transfer on MHD Casson nanofluid past a thin needle. *J. Mol. Liq.* **2019**, 284, 163–174.

26. K. Singh, S.K. Rawat, M. Kumar. Heat and Mass Transfer on Squeezing Unsteady MHD Nanofluid Flow between Parallel Plates with Slip Velocity Effect. *J. Nanosci.* **2016**, 2016 (9708562), 1–11.

27. J. Singh, U.S. Mahabaleshwar, G. Bognár. Mass Transpiration in Nonlinear MHD Flow Due to Porous Stretching Sheet. *Sci. Rep.* **2019**, 9 (1), 1–15,

28. B. Reddappa, M.S. Babu, S. Sreenadh. Magnetohydrodynamic (MHD) Jeffrey Nanofluid Flow over an Exponentially Stretching Sheet through a Porous Medium. *AIP Conf. Proc.* **2023**, 2649, 030003, 1–16,2023.

29. Padmaja. K, R. Kkumar B. Higher order chemical reaction effects on Cu-H2O nanofluid flow over a vertical plate. *Sci. Rep.* **2022**, 12 (1), 17000.

30. K. Padmaja, B. Rushi Kumar. Viscous dissipation and chemical reaction effects on MHD nanofluid flow over a vertical plate in a rotating system. *ZAMM Zeitschrift fur Angew. Math. und Mech.* **2023**, 103 (9), 202200471.

31. N. Sivakumar, B.R. Kumar. Variable conductivity and heat source or sink on MHD unsteady radiated partial slip flow over a sheet with chemical reaction. *AIP Conf. Proc.* **2020**, 2277 (1), 1–10.

32. R. Kumar, K. Gangadhar. Heat generation effects on MHD boundary layer flow of a moving vertical plate with suction. *J. Nav. Archit. Mar. Eng.* **2012**, 9 (2), 153–162.

33. G. Gomathy, B.R. Kumar. Impacts of nanoparticle shapes on Ag-water nanofluid thin film flow through a porous medium with thermal radiation and ohmic heating. *J. Therm. Anal. Calorim.* **2023**, 18, 10 1007 10973–023–12609–.

34. K. Padmaja, B.R. Kumar, O.A. Bég, T.A. Bég. Cross-Diffusion and Higher-Order Chemical Reaction Effects on Hydromagnetic Copper-Water Nanofluid Flow over a Rotating Cone in a Porous Medium. *J. Multiscale Model.* **2023**, 14 (03), 2350006.

35. S. Ravikumar, M. Rafiq, D. Abduvalieva, F.A. Awwad. Effects of Joule heating and reaction mechanisms on couple stress fluid flow with peristalsis in the presence of a porous material through an inclined channel. *Open Phys.* **2023**, 21 (1), 1–16.

36. M.I. Khan, S. Ravikumar, K. Raghunath, et al. Understanding Prandtl fluid flow in conduits with slip boundary conditions: Implications for engineering and physiology. *Phys. Fluids* **2023**, 35 (11), 113106.

37. S. Ravikumar, M. Ijaz Khan, S.A. Alqahtani, S.M. Eldin. Significance of heat and mass transport in peristaltic flow of Jeffrey material subject to chemical reaction and radiation phenomenon through a tapered channel. *Open Phys.* **2023**, 21 (1), 20220258.

38. S. Ravikumar, M. Ijaz Khan, B. Reddappa. The effects of diffusion on the mechanism of peristaltic flow at slip boundaries when internal Joule heating is present. *Heat Transf.* **2023**, 52 (7), 4578–4605.

39. S. Jauhri, U. Mishra. Numerical investigation of MHD nanofluid considering second-order velocity slip effect over a stretching sheet in porous media. *J. Integr. Sci. Technol.* **2023**, 11 (2), 478.

40. S. Ravi Kumar, S.K. Abzal. Combined influence of hall currents and joule heating on hemodynamic peristaltic flow with porous medium through a vertical tapered asymmetric channel with radiation. *Front. Heat Mass Transf.* **2017**, 9 (19), 1–9.

41. S. Ghosh, S. Mukhopadhyay. Some Aspects of Forced Convection Nanofluid Flow over a Moving Plate in a Porous Medium in the Presence of Heat Source/Sink. *J. Eng. Thermophys.* **2019**, 28 (2), 291–304.

42. S. Mukhopadhyay, K. Vajravelu, R.A. Van Gorder. Flow and heat transfer in a moving fluid over a moving non-isothermal surface. *Int. J. Heat Mass Transf.* **2012**, 55 (23–24), 6632–6637.

Journal of Integrated Science and Technology

J. Integr. Sci. Technol., 2024, 12(3), 762   Pg 10